Role of the Coulombic Interaction in Ligand-Induced Biopolymer Aggregation

Norberto Micali,*,† Valentina Villari,† Matteo Cusumano,‡ Maria Letizia Di Pietro,‡ and Antonino Giannetto‡

CNR-Istituto per i Processi Chimico-Fisici, Via La Farina 237, I-98123, Messina, Italy, and Dipartimento di Chimica Inorganica, Chimica Analitica e Chimica Fisica Università di Messina, C.da Papardo S.ta Sperone 31, I-98166, Messina, Italy

Received: September 6, 2006; In Final Form: November 23, 2006

The interaction mechanisms responsible for the binding between metal complexes and biopolymers in aqueous solution, as well as the consequent aggregation process of biopolymers themselves, involve many factors, from geometrical aspects and hydrophobic contributions, as examples, to the electrostatic potential. In this paper aqueous solutions of a polynucleotide, polyadenylic acid (PolyA), which mimics the helix arrangement of RNA or single-stranded DNA but has a simpler structure, are used as a model system. The role of the electrostatic interactions in the binding process between some platinum(II) complexes and PolyA and in the aggregation among PolyA molecules is investigated, by means of elastic and quasielastic light scattering and electrophoretic mobility. The results show that the presence of large, planar aromatic moiety in the dicationic platinum(II) complexes is essential for the binding with PolyA and suggest that the consequent lowering of the local electrostatic barrier between PolyA molecules can be involved in triggering the aggregation process.

I. Introduction

The interaction of DNA or RNA with planar metal complexes containing aromatic ligands has been an active research area during the last 20 years. Metal ions are present in practically all biological systems and can stabilize or destabilize biological structures.[1−3] Metal-ion interaction with nucleic acids plays an important role in different biological processes such as genetic expression, metalloenzymatic processes, mutagenesis, carcinogenesis, and DNA packing in living cells.[4−7] Some platinum metallodrugs, for instance, bind to DNA through covalent interactions and have proved to be among the most effective pharmaceuticals used to treat cancers.[8,9]

Nevertheless, one of the most important targets in designing new drugs is that they act specifically, and this specificity is founded mainly on noncovalent binding. The intercalation is one example of noncovalent interaction which depends on many factors such as planarity and aromaticity as well as surface extension of the interacting group. Molecules bearing aromatic coplanar groups are potential DNA intercalators,[10−13] and, in particular, this binding mode has been suggested for some cationic platinum(II) complexes.[14−21] Nevertheless, the binding between charged metal-containing ligand and DNA can involve many interactions and give rise to complex processes[22] so that the subject is still somehow controversial.

In contrast to the numerous studies on the binding mechanisms of drugs to double stranded DNA, the interaction with single stranded RNA is a subject which has been developing since the past decade only. The main reason is related to the more complex structure of RNA which is able to fold forming regions with double stranded structure.

Recently,[23,24] it has been put in evidence that the single stranded Polyadenilic acid present in the tail of RNA is fundamental for the stability of cells and transcription processes; thus, the study of the interaction of drugs with single stranded RNA by specific binding or intercalation opens new perspectives toward more effective therapies.[24,25]

In this paper aqueous solutions of the polynucleotide polyadenylic acid (PolyA) are used as a model system (a simpler structure than single-stranded DNA/RNA) to investigate, by means of elastic and quasielastic light scattering and electrophoretic mobility, the role of the electrostatic interactions in the binding process between platinum(II) complexes and the biopolymer.

Compared with neutral polymers, the structure and dynamics of charged polymers in solution, like PolyA, are not fully understood yet, and molecular interpretations of the experimental results are still, in many cases, a subject of scientific debate. This is mainly due to the charge effect which depends strongly on the ionic strength of the solution, as well as to the hydrodynamic interaction effect on the dynamical properties; the latter, in their turn, depend on the chain conformation. Theoretical and experimental studies on polyelectrolyte solutions are richly documented in the literature (see for example references 26−31 and citations therein) in a wide range of concentration, molecular weight, and ionic strength.

The aim of the present paper is to investigate the binding phenomenon between platinum(II) complexes and PolyA. It will be shown that a specific interaction exists which gives rise to the binding between aromatic-containing metal complexes and PolyA. The electrostatic contribution is likely involved successively, through the lowering of the energy barrier between PolyA molecules, and it can be responsible for the extensive aggregation. Such an induced aggregation phenomenon can assume an important role as suppressor of DNA/RNA functionality in addition to that of intercalation.

II. Experimental Section

A. Material. Polyadenylic acid (PolyA), purchased by Amersham Biosciences, was investigated in a freshly prepared

* Corresponding author. E-mail: micali@me.cnr.it. Phone: +39 090 2939693. Fax: +39 090 2939902.
† CNR-Istituto per i Processi Chimico-Fisici.
‡ Università di Messina.

10.1021/jp065795w CCC: $37.00
Published on Web 01/17/2007

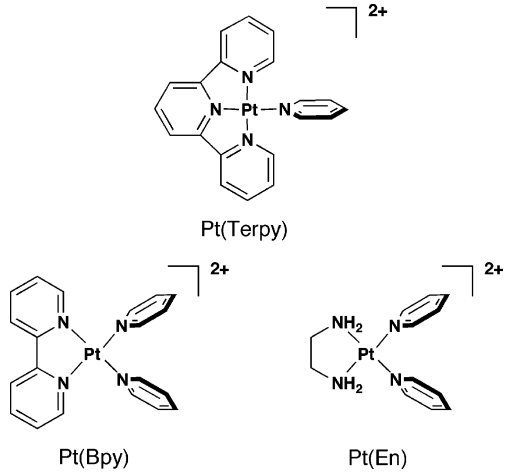

Figure 1. Formulas and abbreviations of the complexes used: Pt(Terpy) = $[Pt(terpy)(py)]^{2+}$; Pt(Bpy) = $[Pt(bpy)(py)_2]^{2+}$; Pt(En) = $[Pt(en)(py)_2]^{2+}$.

water solution at a concentration of 2.1×10^{-5}g/cm^3 (60 μM in bases, Adenine). As it will be shown in the discussion section, this concentration value lies in the dilute regime.

Dicationic Platinum(II) Complexes: $[Pt(terpy)(py)](BF_4)_2$,[32] $[Pt(bpy)(py)_2](PF_6)_2$,[33] and $[Pt(en)(py)_2](PF_6)_2$[34] (terpy = 2,2′:6′,2″-terpyridine; bpy = 2,2′-bipyridine; py = pyridine; en = ethylenediamine) were prepared as described in the literature. $[Pt(bpy)(py)_2]^{2+}$ differs from $[Pt(terpy)(py)]^{2+}$ for the surface extension of the planar aromatic moiety, while $[Pt(en)(py)_2]^{2+}$ differs for the absence of any aromatic group in the coordination square plane of the metal (see Figure 1).[35]

The dicationic platinum(II) complexes were added to the PolyA solution and different samples were prepared at different molar ratios [complex]/[PolyA]. The molar concentration of PolyA indicates the molar content of its bases.

All the solutions were buffered with a 1 mM phosphate buffer at pH = 7, and sodium nitrate[36] was added to obtain a total ionic strength of 11 mM. The pH was measured with a Radiometer PHM 62.

$NaNO_3$ and other chemicals were of reagent grade and were used without further purification.

B. Method. Light scattering experiments were performed by using a Nd:yttrium−aluminum garnet laser source (λ = 532 nm) at a power of 100 mW, linearly polarized orthogonally to the scattering plane, and a homemade computer controlled goniometric apparatus which collected the scattered light in a pseudo-cross correlation mode (through two cooled R942-02 photomultipliers at the same scattering angle). To measure the depolarization ratio, a Glan−Taylor polarizer was placed in the incident laser path and a Glan−Thomson analyzer in the scattered beam. The temperature was controlled by a homemade water-circulating apparatus which provided a constant temperature of 25 ± 0.01 °C.

For the dynamic-light scattering measurements, the scattered light, collected in a self-beating mode, is analyzed by a MALVERN 4700 correlator which builds up the normalized intensity autocorrelation function:[37,38]

$$g_2(Q,t) = \frac{\langle I(Q,0)\, I(Q,t)\rangle}{\langle I(Q)\rangle^2} \tag{1}$$

where $|Q| = (4\pi n/\lambda)\sin(\theta/2)$ (θ being the scattering angle, n the refractive index of the medium, and λ the wavelength of light in vacuum).

For diffusing monodisperse spherical scatterers with hydrodynamic radius R_H (such as $QR_H \ll 1$), the normalized intensity autocorrelation function takes a simple exponential form, $g_2(Q, t) = 1 + \exp(-2\Gamma t)$ with $\Gamma = DQ^2$ (D being the collective diffusion coefficient). Because the investigated solutions are slightly polydisperse, the autocorrelation functions have been analyzed in terms of a standard cumulant analysis[37−39] to find a mean diffusion coefficient, D_{eff}.

For the static light-scattering measurements, the scattered intensity profile of the solution is corrected for the solvent contribution and then normalized by the absolute scattered intensity of toluene used as reference. The absolute scattered intensity can be written as[37−39]

$$I(Q) = KM_W c\, P(Q)\, S(Q) \tag{2}$$

$P(Q)$ and $S(Q)$ being the normalized form factor and the structure factor, respectively, M_w is the molecular weight, c *is* the mass concentration, and K is the optical constant. For the scattering geometry of the experiment, it is

$$K = \frac{4\pi^2 n^2}{\lambda^4 N_A}\left(\frac{dn}{dc}\right)^2 \tag{3}$$

It can be considered that, for the solutions investigated, the concentration is low enough that the mean diffusion coeficient D_{eff} can be identified with the diffusion coefficient at infinite dilution ($D_0 = k_B T/(6\pi\eta R_H)$, k_B being the Boltzmann's constant, T the absolute temperature, and η the solvent viscosity) and $S(Q)$ can be approximated to unity.

The electrophoretic mobility, μ, of the particles was measured by the Brookhaven Zeta-PALS instrument, which is based on the principles of phase-analysis light scattering. The laser light (λ = 661 nm) is split before impinging on the sample: a portion passes through the sample which is placed in an oscillating electric field; the other portion of the beam is used as reference, modulated at 250 Hz and then recombined with the scattered beam. This geometry allows for measuring even a small deviation of the frequency in the scattered light by performing a phase comparison between the detected signal and the imposed frequency. If a small mobility is present, $\mu = \mathbf{v}/\mathbf{E}$ ($\mathbf{v}$ being the velocity of the charged particles under the electric field $\mathbf{E}$), the phase change can be measured by a phase comparator. The amplitude-weighted phase difference, AWPD, can be written as:[40]

$$\langle\phi(t) - \phi(0)\rangle = \langle A\rangle Q[\mu\, E(t) + V_c t] \tag{4}$$

where $\langle A\rangle$ is the amplitude of the Doppler signal, Q the exchanged wavevector and V_c is a constant taking into account collective motions due to eventual temperature gradients. Typical value of the applied electric field amplitude used in the experiment is 7 V/cm. The value of mobility was extracted by using the Zeta-PALS software by Brookhaven.

III. Results

The presence of the Pt(Terpy) complex in a PolyA dilute solution induces an aggregation phenomenon in the investigated solutions. Upon the addition of the Pt(Terpy) complex to the PolyA aqueous solution and upon increasing the Pt(Terpy) complex concentration (PolyA concentration is fixed), the scattered intensity at 90° is almost constant below the molar ratio n_{Pt}/n_{PolyA} = 0.4. Above this value it increases monotonically, as shown in Figure 2. Because the intensity of the Pt(Terpy) complex alone in aqueous solution at the highest

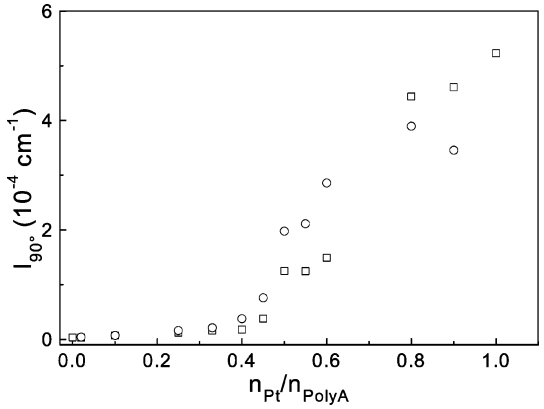

Figure 2. Absolute scattered intensity of fresh (squares) and 4 h aged (circles) solutions as a function of Pt(Terpy)/PolyA molar ratio.

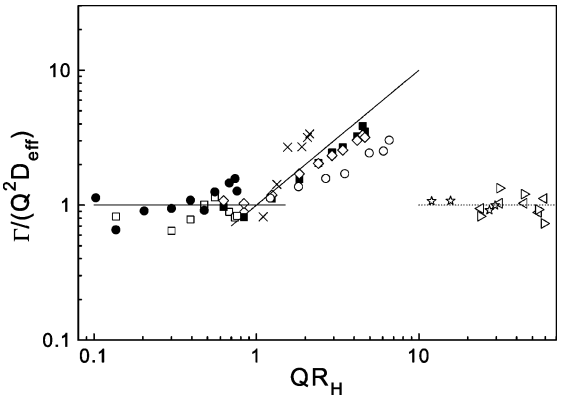

Figure 3. Normalized relaxation rate for PolyA (hollow squares) and for Pt(Terpy)/PolyA solutions (stabilized for 4 h) at different molar ratios: 0.25 (filled circles), 0.4 (crosses), 0.5 (filled squares), 0.55 (diamonds), 0.6 (circles), 0.8 (left triangles), 0.9 (right triangles), and 1 (stars). The straight lines indicate the Q^2 and Q^3 regime.

concentration investigated (60 μM) is comparable to that of PolyA, the observed increase of intensity can be addressed to the aggregation.

The scattered intensity increases rapidly within a few minutes from the mixing of reagents owing to the aggregation process, but thereafter it increases slowly. Figure 2 reports a comparison between the intensity collected from the freshly prepared solutions and from the 4 h aged ones. However, by monitoring the changes in the scattered light, it is found that, for the solutions with a molar ratio lower than 0.5, the scattered intensity does not vary anymore after a few minutes from mixing, whereas, for those above 0.5, it continues to increase upon aging. In particular, for a molar ratio above 0.8, solutions undergo flocculation after about 8 h, indicating the presence of aggregates with micrometric size. However, also for these solutions the scattered intensity changes slowly enough to ensure the stability during the measurement.

To obtain the aggregate size from the dynamic light scattering, the correlation function has been measured at different scattering angles for all the molar ratios. Figure 3 displays the normalized relaxation rates obtained after 4 h from mixing, by using the cumulant expansion truncated at the third order.[37−39] For PolyA and Pt(Terpy)/PolyA solution at a molar ratio lower than 0.4 and from 0.8 to 1, the Q^2-dependence of Γ is fulfilled. On the other hand, in the range of molar ratio between 0.4 and 0.6 the relaxation rate displays a Q^3-behavior.

In the range 0.4−0.6 no diffusion coefficient can be extracted from the whole Q-dependence of the relaxation rate, because of the existence of internal motions along with the Brownian

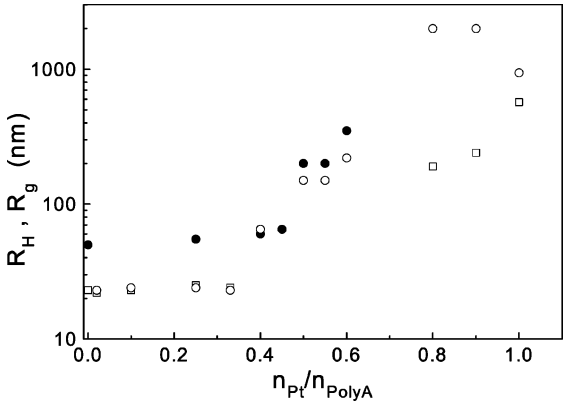

Figure 4. Hydrodynamic radius (hollow symbols) and radius of gyration (filled symbol) of the aggregates present in the fresh (squares) and aged (circles) solutions.

diffusion. However, at the lowest Q values, Γ/Q^2seems to reach a plateau which reasonably indicates the value of the diffusion coefficient. Data are normalized by the diffusion coefficient and reported as a function of QR_H.

The polydispersity of the PolyA solution in the absence of Pt complexes is lower than 10%, whereas in the presence of the Pt(Terpy) complex polydispersity increases up to 20−25%.

In Figure 4 the hydrodynamic radius of the aggregates (hollow symbols) is reported for fresh and aged solutions. As it can be seen, below the molar ratio 0.4 the hydrodynamic radius is almost constant at about 25 nm and equal to that of PolyA; also the aging does not affect particle size. Above 0.8 the hydrodynamic radius of the aggregate in the fresh solutions is about 200 nm and reaches the value of about 500 nm at the molar ratio 1; however, in a couple of hours aggregates reach a micrometric size. In the molar ratio range above 0.8, the condition $QR_H \ll 1$ is certainly not fulfilled, so that the Q^2-dependence of Γ suggests that the aggregates, although micrometric in size, are quite rigid.

In order to estimate the radius of gyration of the aggregates, especially in the region of internal mobility, the intensity profiles have been measured. As reported in Figure 5a, the intensity profile of PolyA and of Pt(Terpy)/PolyA solutions below the molar ratio 0.45 obeys a Guinier law:

$$P(Q) = \exp\left(-\frac{Q^2R_g^2}{3}\right) \qquad (5)$$

where R_g is the radius of gyration of the particle.

The intensity profile is the same for PolyA and Pt(Terpy)/PolyA solutions below the molar ratio 0.25 and gives the value of about 50 nm for the radius of gyration (the dotted part of the fitting lines in Figure 5a indicates the $QR_g > 1$ region). From the molar ratio 0.25 to 0.45, the radius of gyration does not seem to increase significantly (as found for R_H).

The intensity profile starts to change at the molar ratio 0.5; the Guinier law is not obeyed anymore ($QR_g \gg 1$), and a model for the form factor of the particle in needed.

The ratio $\rho = R_g/R_H \approx 2$ found at low molar ratios can indicate a rodlike or a random coil ($\rho = 1.8 \div 2$) conformation of the particles. The very low depolarization ratio of the scattered beam ($I_{VH}(Q)/(I_{VV}(Q) - {}^4/_3 I_{VH}(Q)) \approx 0.001$, I_{VV} and I_{VH} being the polarized and depolarized scattered intensity, respectively) for all molar ratios suggests rather a random coil conformation. PolyA can assume such a conformation because of the ionic strength of the solution, which provides a partial screening of the repulsion between monomers and allows for the chain flexibility.

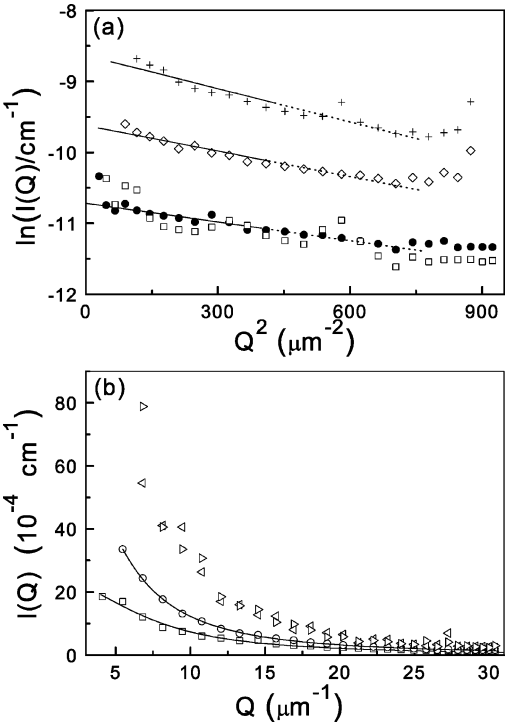

Figure 5. (a) Intensity profiles of PolyA (squares) and Pt(Terpy)/PolyA at molar ratio 0.25 (filled circles), 0.4 (diamonds), and 0.45 (crosses). The straight lines are the fit accoding to the Guinier law. (b) Intensity profiles of Pt(Terpy)/PolyA at molar ratio 0.5 (squares), 0.6 (circles), 0.8 (right triangles), and 0.9 (left triangles). The continuous lines are the fit according to the Debye form factor (eq 6).

In Figure 5b the intensity profiles for the solutions at molar ratio above 0.45 are reported along with the fit obtained by using the Debye form factor (for the solutions at 0.5 and 0.6 molar ratios as examples), which describes the random coil conformation:

$$P(Q) = \frac{[\exp(-Q^2R_g^2) - 1 + Q^2R_g^2]}{(QR_g)^4} \qquad (6)$$

The obtained radius of gyration increases (see Figure 4) to about 200 nm and appears to increase further above the molar ratio 0.6. The ionic strength of the solution could also suggest the use of the sphere form factor to take into account the possibility of a globular conformation; however, such an approach is not consistent with the experimental data. This occurrence is likely because the ionic strength is not high enough.

The fitting of the intensity profiles of solutions at a molar ratio of 0.8−1 with the Debye relation leads to a radius of gyration of about 1 μm. However, it is possible that this value is underestimated because the Q region investigated is too high for evaluating the size on a micrometric scale. In fact, as shown in Figure 6, by plotting the data in a log−log scale, it appears that, whereas the profile of the solution at 0.6 still bends at lower Q values, that of the solutions above 0.8 displays a power law with exponent −2.3. In particular, the small angle ($Q < 5\mu m^{-1}$) scattered intensity of the sample at molar ratio 1 has the same slope as in the high Q region with no bending, thus indicating that the aggregates certainly have a radius larger than 1.5 μm.

According to the theoretical description of fractals,[41,42] they obey the power law $I(Q) \propto Q^{-D_f}$, D_f being the fractal dimension. For kinetic mechanisms of growth driven by the diffusion coefficient, it holds $1.75 \leq D_f \leq 2.5$. The value of 2.3, found

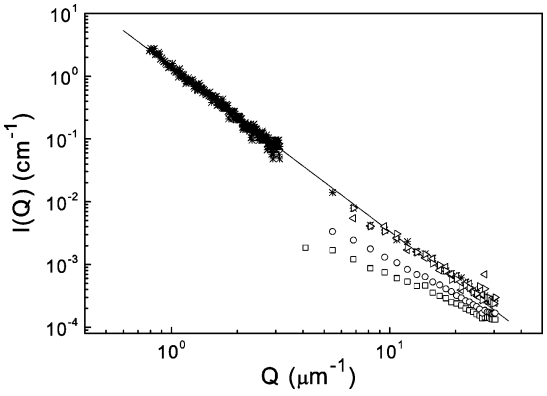

Figure 6. The intensity profile of the Pt(Terpy)/PolyA solution at molar ratio 1 (stars) is reported together with the data at small angle (for comparison, data at 0.5 (squares), 0.6 (circles), 0.8 (right triangles), and 0.9 (left triangles) molar ratios are also reported). The straight line is the fit according to a power law.

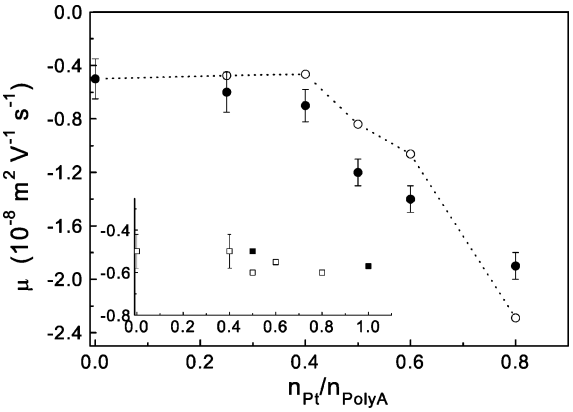

Figure 7. Electrophoretic mobility at different amounts of Pt(Terpy) complex (filled circles); the hollow circles represent the theoretical value according to the model described in the text (the dotted line is a guide for eye). The insert reports the measured electrophoretic mobility of PolyA in the presence of Pt(Bpy) (hollow squares) and of Pt(En) (filled squares).

for solutions at the highest molar ratios, is in between the fractal dimension of a reaction limited cluster aggregation (RLCA) ($D_f = 2.1$) and a diffusion-limited aggregation (DLA) ($D_f = 2.5$) mechanism. The same fractal arrangement inside the aggregate is observed for lower molar ratio (0.45) with an ionic strength ten times higher (data not shown).

The fact that PolyA molecules tend to aggregate even in the presence of an excess of positive charge seems to suggest that the interaction between PolyA and the Pt(Terpy) complex is not merely electrostatic. The measure of the electrophoretic mobility should help to clarify this point. The net charge of PolyA molecules in aqueous solution is negative and corresponds to a small mobility value of about -0.5×10^{-8} m^2 V^{-1} s^{-1} (see Figure 7). On increasing the amount of the Pt(Terpy) complex, the electrophoretic mobility slowly decreases for molar ratios below 0.4. Above this value, which corresponds to the beginning of an extensive aggregation (see Figure 4), it becomes significantly more and more negative. This result implies that aggregation occurring among PolyA molecules is not induced merely by the balance of their negative charge. In order to prove further that a specificity must exist in the interaction between PolyA and the Pt(Terpy) complex, two different complexes are used: Pt(Bpy), which has a smaller extension of the planar aromatic moiety than Pt(Terpy), and Pt(En) which does not bear any aromatic coplanar rings.

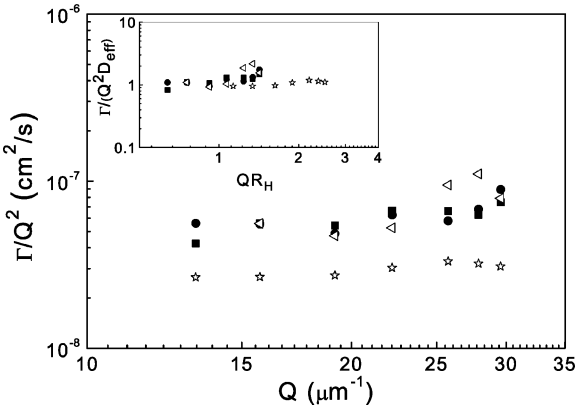

Figure 8. Relaxation rate of Pt(Bpy)/PolyA at different molar ratios: 0.25 (filled circles), 0.5 (filled squares), 0.8 (left triangles), and 1 (stars). In the inset the corresponding normalized data are reported.

The inset of Figure 7 shows that electrophoretic mobility is almost constant in the entire molar ratio range from 0 to 1. Moreover, the light scattering measurements show a weak tendency to aggregation for the Pt(Bpy)/PolyA system and no aggregation for the Pt(En)/PolyA one.

In particular, the decay rate of the correlation function of Pt(Bpy)/PolyA (4 h aged solutions) seems to displays a Q^3 dependence in the molar ratio range 0.4−0.6, whereas it obeys a diffusion law at 0.8 (as shown in Figure 8), in analogy to the Pt(Terpy)/PolyA solutions. However, in this case, the hydrodynamic radius increases from 25 to 50 nm for molar ratios below 0.6 and to 75 nm at 0.8. These values are much smaller than that obtained by adding the Pt(Terpy) complex at the same molar ratio.

IV. Discussion

The aggregation phenomenon of PolyA is induced by the presence of the Pt(Terpy) complex, it is triggered above the molar ratio 0.4, and it is faster as the molar ratio increases. Below this value, both the PolyA size and intensity profile do not seem to depend either on molar ratio or on time. The intensity value of the PolyA solution extrapolated to $Q = 0$ gives the molecular weight value (through relation 2) $M_W \approx 3.5 \times 10^5$. By using this value, it is possible to calculate the overlap concentration c^* which defines the crossover between the dilute and the semidilute regime:[43,44] $c^* = 3M_W/(4\pi N_A R_g^3) \approx 10^{-3}$g/cm^3. The concentration of PolyA used in this work, much lower than c^*, ensures that the system is in the dilute regime even for the aggregated PolyA (the fractal dimension suggests that the mass of the aggregate scales with its size through a power higher than 2).

The clear change in the overall intensity observed in the molar ratio range of 0.35−0.45 could be ascribed to the increased dn/dc value owing to the presence of the Pt(Terpy) complex in the PolyA molecules; the radius of gyration of PolyA, in fact, does not change significantly in this molar ratio range.

The irreversible aggregation process occurring above the molar ratio 0.4 could be ascribed to both local charge neutralization and a specific interaction of Pt(Terpy) complex linking two PolyA molecules (physical cross-linking). The comparison between light scattering and electrophoretic mobility data of three complexes with different structures and the same electric charge would suggest that the electrostatic contribution does not play the main role.

In an aggregation process induced be a mere electrostatic interaction, a decrease of the absolute value of the macromolecule electrophoretic mobility (and therefore its net charge) should be expected upon increasing the molar ratio of the species with opposite charge.[45] On the other hand, it seems that the presence of the aromatic rings is essential to induce the aggregation process and that, unlike the other two complexes, the peculiar structure of Pt(Terpy) is able to give rise to a physical cross-linking effect between PolyA molecules.

At low molar ratios the cross-linking probability is too small to produce extended aggregation. In the molar ratio range between 0.4 and 0.6 the cross-linking probability increases and the structure of the aggregate can be sketched as a flexible network whose contact points are constituted by the Pt(Terpy) complex molecules. Flexibility is suggested by the Q^3-dependence of the correlation function relaxation rate. At higher molar ratios the high contact point density, which constraints conformational rearrangements, makes the network rigid as suggested by the Q^2-dependence of the correlation function relaxation rate.

To measure the net charge, a transference experiment[46,47] should be performed. However, the results obtained by the electrophoretic mobility can give useful information when only a qualitative relation between mobility and net charge is required. The understanding of the electrophoretic mobility data for polyelectrolyte solutions is more complex than for colloids. For the latter the concept of the ζ-potential (i.e., the electrostatic potential at the shear plane where the liquid velocity is zero) can be introduced and related to the electrophoretic mobility.[48−52] In the case of a dilute polyelectrolyte solution, mobility can be written as:[28]

$$\mu = \frac{qD_0}{k_B T} N(\kappa R_g) \tag{7}$$

where, for any κR_g value,

$$N(\kappa R_g) = \frac{2R_g}{\pi} \int_0^\infty \frac{Q^2}{Q^2 + \kappa^2 R_g^2} P(Q)\, dQ \tag{8}$$

Therefore, mobility depends on the molecular weight of the polyelectrolyte, M_W, through the net charge (linearly) and through the scaling laws of $D_0 \propto R_g^{-1} \propto M_W^{1/d}$ and $N(\kappa R_g)$ (d being the dimensionality of the aggregate). Only in the limits $\kappa R_g \ll 1$ and $\kappa R_g \gg 1$ do the form of eq 8 and the scaling laws between static and dynamic quantities ensure that mobility is independent of molecular weight;[28] this occurrence does not allow for relating the mobility with the net charge directly.

In the following, the aggregates of PolyA will be considered as polyelectrolytes with different molecular weight (mM_W, m being the number of PolyA molecules in the aggregate) and with net charge $q = mq_0(1 - 2(n_{Pt}/n_{PolyA})\varphi)$, q_0 being the charge of PolyA and φ the fraction of Pt(Terpy) complex molecules linked to PolyA. Because of the increase of R_g as a function of molar ratio, κR_g fulfills the limit condition $\kappa R_g \gg 1$ only for high molar ratios; so that the general form of eq 8 should be used to sketch the overall behavior of the electrophoretic mobility as a function of the molar ratio between metal−complex and PolyA. By exploiting the static scaling law $m \propto R^d$, the electrophoretic mobility (eq 7) takes the form

$$\mu = C\left[R_g^{d-1}\left(1 - 2\frac{n_{Pt}}{n_{PolyA}}\varphi\right)\right] N(\kappa R) \tag{9}$$

where C is a constant such as $\mu = \mu_0$ for $(n_{Pt}/n_{PolyA}) = 0$, μ_0 being the mobility of PolyA in the absence of the Pt(Terpy) complex.

The result obtained by using eq 9, in which we put $d = 2.5$, $\varphi = 0.2$, and $P(Q)$ the Debye form factor (eq 6), is plotted (hollow circles) in Figure 7, together with the experimental data (filled circles). It is worth noting that this approach requires not only that the Debye form factor is valid in all the molar ratio range but also that the dimensionality, d, of the aggregate is a constant (one evident consequence of the roughness of such an approximation is already evident from the fact that the Debye form factor would imply the value $d = 2$ in eq 9). From the extensive literature on polyelectrolyte solutions it is known that these conditions are not always satisfied and that the chain conformation depends crucially on intramolecular interaction through many factors, like counterion distribution around chains, shielded electrostatic potential, hydrophobic contribution and so on.[53] However, by considering the approximation involved in this simple model, which only aims to describe the main features of the complex interactions involved in the system, the obtained value of the dimensionality of the aggregate agrees well with that resulting by the measurement of the intensity profiles at high molar ratio ($D_f = 2.3$). As above stressed, this value lies in the range between the fractal dimensions of RLCA and DLA fractals. This occurrence is sometimes encountered experimentally[54,55] and was explained by some authors[56] who showed that the measured fractal dimension of a diffusion-limited cluster−cluster aggregation and reaction limited cluster aggregation growth mechanism is an increasing function of the building blocks asymmetry. As in an aqueous solution at pH = 7, PolyA is a single helix,[1] the distinction between the two kinetic mechanisms of growth can be lost.

The value of 0.2 for the fraction of Pt(Terpy) complex molecules linked to PolyA would suggest that only a part of the total amount of Pt(Terpy) complex molecules is involved in the interaction with PolyA molecule. By using the same model for the less interacting Pt(Bpy) complex (possessing the same charge as the Pt(Terpy) complex), the electrophoretic mobility data are reproduced satisfactorily by putting $\varphi = 0$ and $d = 2$ (the latter being in agreement with the Debye form factor).

Therefore, the effect of the Pt(Terpy) complex is to interact with PolyA specifically and successively to induce aggregation more rapidly than the balance of the overall charge of the molecule. This physical cross-linking effect can be addressed to a local charge neutralization which lowers the repulsive energy barrier between different PolyA molecules. The fact that the electrostatic attraction between Pt complex molecules and PolyA does not play the main role could be due to the ionic strength which acts to screen the charge.

V. Conclusions

By comparing the results obtained by light scattering and electrophoretic mobility measurements in aqueous solutions of PolyA in the presence of dicationic platinum(II) complexes, it emerges that the electrostatic contribution from the dicationic charge of the metal-ligands does not play any role in the binding process with PolyA. Rather, the surface extension of the aromatic moiety in the coordination plane of the metal is responsible for the binding (and binding efficacy) with PolyA. This occurrence appears to be consistent with the intercalation phenomenon suggested in literature as the binding mechanism with DNA/RNA.[14−21,24,25]

The role of the Pt(II) complex interacting with PolyA can be sketched as a physical cross-linking between different biopolymers, and this effect could be driven mainly by specific interactions. On the other hand, the electrostatic interaction could be involved in the successive irreversible extended aggregation of PolyA, owing to the local charge neutralization of some part of the PolyA molecule.

To make this description more quantitative, a model which accounts for the dependence of the net charge of the aggregates and their size on the molar fraction of the complex has been introduced. The results of this modeling indicate that, whereas in the solution with Pt(Bpy) and Pt(En) complexes there is a negligible percentage of complex molecules involved in the interaction with PolyA and belonging to the aggregate, in the case of the Pt(Terpy) complex this percentage is about 20%. Therefore, the higher binding efficacy of the latter complex in interacting specifically with PolyA induces, through a cross-linking, the biopolymer aggregation more rapidly than the balance of the overall charge of the molecule (likely by decreasing locally the electrostatic energy barrier).

The knowledge of selective binding processes to biopolymers and the induction of aggregation is fundamental in establishing a basis for designing molecules with specific properties to be used in biological and pharmaceutical sciences.

Supporting Information Available: Graphs showing the dependence of the relaxation rate on the exchanged wave vector for PolyA and for Pt(Terpy)/PolyA solutions and the magnified view of Figure 3. This material is available free of charge via the Internet at http://pubs.acs.org.

References and Notes

(1) Saenger, W. *Principles of Nucleic Acid Structure*; Springer-Verlag: New York, 1984.
(2) Semenov, M. A.; Bol'bukh, T. V.; Kashpur, V. A.; Maleev, V. Y.; Mrevlishvili, G. M. *Biofizika* **1994**, *39*, 50.
(3) Iyer, H. V.; Przybycien, T. M. *J. Colloid. Interface Sci.* **1996**, *177*, 391.
(4) Izatt, R. M.; Christensen, J. J.; Rytting, J. H. *Chem. Rev.* **1966**, *66*, 439.
(5) Lerman, L. S. *Cold Spring Harbor Symp. Quant. Biol.* **1973**, *38*, 59.
(6) Sissoeff, I.; Grisvard, J.; Guille, E. *Prog. Biophys. Mol. Biol.* **1976**, *31*, 165.
(7) Bloomfield, V. A. *Biopolymers* **1998**, *44*, 269.
(8) Reedijk, J. *Chem. Commun.* **1998**, 801 and references therein.
(9) Guo, Z. J.; Sadler, P. J. *Adv. Inorg. Chem.* **2000**, *49*, 183 and references therein.
(10) Barton, J. K.; Danishefsky, A. T.; Goldberg, J. M. *J. Am. Chem. Soc.* **1984**, *106*, 2172.
(11) Barton, J. K.; Goldberg, J. M.; Kumar, C. V.; Turro, N. J. *J. Am. Chem. Soc.* **1986**, *108*, 2081.
(12) Hiort, C.; Lincoln, P.; Nordèn, B. *J. Am. Chem. Soc.* **1993**, *115*, 3448.
(13) Dupureur, C. M.; Barton, J. K. *Inorg. Chem.* **1997**, *136*, 33.
(14) Lippard, S. J. *Acc. Chem. Res.* **1978**, *11*, 211.
(15) Sundquist, W. I.; Lippard, S. J. *Coord. Chem. Rev.* **1990**, *100*, 293.
(16) Barton, J. K.; Lippard, S. J. *Biochemistry* **1979**, *18* 2661.
(17) Cusumano, M.; Di Pietro, M. L.; Giannetto, A.; Nicoló, F.; Rotondo, E. *Inorg. Chem.* **1998**, *37*, 563.
(18) Cusumano, M.; Di Pietro, M. L.; Giannetto, A. *Inorg. Chem.* **1999**, *38*, 1754.
(19) Liu, H.-Q.; Peng, S.-M.; Che, C. M. *Chem. Commun.* **1995**, 509.
(20) Che, C. M.; Yang, M.; Wong, K.-H.; Chan, H.-L.; Lam, W. *Chem.—Eur. J.* **1999**, *5*, 11.
(21) McCoubrey, A.; Latham, H. C.; Cook, P. R.; Rodger, A.; Lowe, G. *FEBS Lett.* **1996**, *380*, 73.
(22) Cusumano, M.; Di Pietro, M. L.; Giannetto, A. *Inorg. Chem.* **2006**, *45*, 230.
(23) Wickens, M.; Andersont, P.; Jackson, R. J. *Curr. Opin. Genet. Dev.* **1997**, *7*, 220.
(24) Giri, P.; Hossain, M.; Kumar, G. S. *Bioorg. Med. Chem. Lett.* **2006**, *16*, 2364 and references therein.
(25) Piantanida, I.; Palm, B. S.; Cudiè, P.; Zinič, M.; Schneider, H.-J. *Tetrahedron* **2004**, *60*, 6225.
(26) Schmitz, K. S. *Macroions in Solution and Colloid Suspension*; VCH: New York, 1993.
(27) Fitch, R. M. *Polymer Colloids: A comprehensive introduction*; Academic Press: London, 1997.
(28) Muthukumar, M. *J. Phys. Chem.* **1997**, *107*, 2619.

(29) Liu, H.; Skibinska, L.; Gapinski, J.; Patkowski, A.; Fischer, E. W.; Pecora, R. *J. Chem. Phys.* **1998**, *109*, 7556.
(30) Ermi, B. D.; Amis, E. J. *Macromolecules* **1997**, *30*, 6937.
(31) Matsuoka, H.; Ise, N.; Okubo, T.; Kunugi, S.; Tomyiama, H.; Yoshikawa, Y. *J. Chem. Phys.* **1985**, *83*, 378.
(32) Lowe, G.; Vilaivan, T. *J. Chem. Res., Synop.* **1996**, 386.
(33) Cusumano, M.; Di Pietro, M. L.; Giannetto, A. *Chem. Commun.* **1996**, 2527.
(34) Appleton, T. G.; Hall, J. R. *Inorg. Chem.* **1971**, *10*, 1717.
(35) All the complexes were characterized by elemental analysis and ^{1}H NMR.
(36) Cusumano, M.; Di Pietro, M. L.; Giannetto, A.; Romano, F. *Inorg. Chem.* **2000**, *39*, 50.
(37) Berne, B. J.; Pecora, R. *Dynamic Light Scattering*; Wiley-Interscience: New York, 1976.
(38) *Light Scattering: Principles and Development*; Brown, W., Ed.: Clarendon: Oxford, 1996.
(39) Chu, B. *Laser Light Scattering-Basic Principle and Practice*, 2nd ed.; Academic: San Diego, CA, 1991.
(40) Miller, J. F.; Schätzel, K.; Vincent, B. *J. Colloid. Interface Sci.* **1991**, *143*, 532.
(41) Stanley, H. E.; Ostrowsky, N. *On Growth and Form*; NATO ASI Series; Martinus Nijhoff: Dordrecht, The Netherlands, 1986.
(42) Mallamace, F.; Micali, N.; Trusso, S.; Monsù Scolaro, L.; Romeo, A.; Terracina, A. *Phys. Rev. Lett.* **1996**, *76*, 4741.
(43) Brown, W.; Nicolai, T. In *Dynamic Light Scattering: The method and some application*; Brown, W., Ed.: Clarendon Press: Oxford, 1993.
(44) Micali, N.; Villari, V. *Phys. Rev. E* **2003**, *67*, 41401.
(45) Yu, X.; Somasundaran, P. *J. Colloid Interface Sci.* **1996**, *177*, 283.
(46) Huizenga, J. R.; Grieger, P. F.; Wall, F. T. *J. Am. Chem. Soc.* **1950**, *72*, 2636.
(47) Ito, K.; Ise, N.; Okubo, T. *J. Chem. Phys.* **1985**, *82*, 5732.
(48) Delgado, A. V.; González-Caballero, F.; Hunter, R. J.; Koopal, L. K.; Lyklema, J. *Pure Appl. Chem.* **2005**, *77*, 1753.
(49) McNeil-Watson, F.; Tscharnuter, W.; Miller, J. *Colloids Surf., A* **1998**, *140*, 53.
(50) Hunter, R. J. *Foundations of Colloid Science*; Oxford University Press: NewYork, 1986; Vols. I−II.
(51) Micali, N.; Villari, V.; Consoli, G. M. L.; Cunsolo, F.; Geraci, C. *Phys. Rev. E* **2006**, *73*, 51904.
(52) Crocker, J. C.; Grier, D. G. *Phys. Rev. Lett.* **1996**, *77*, 1897.
(53) Liu, S.; Muthukumar, M. *J. Chem. Phys.* **2002**, *116*, 9975.
(54) Micali, N.; Villari, V.; Mineo, P.; Vitalini, D.; Scamporrino, E.; Crupi, V.; Majolino, D.; Migliardo, P.; Venuti, V. *J. Phys. Chem. B* **2003**, *107*, 5095.
(55) Micali, N.; Villari, V.; Castriciano, M. A.; Romeo, A.; Monsù Scolaro, L. *J. Phys. Chem. B* **2006**, *110*, 8289.
(56) Mohraz, A.; Moler, D. B.; Ziff, R. M.; Solomon, M. J. *Phys. Rev. Lett.* **2004**, *92*, 155503-1.